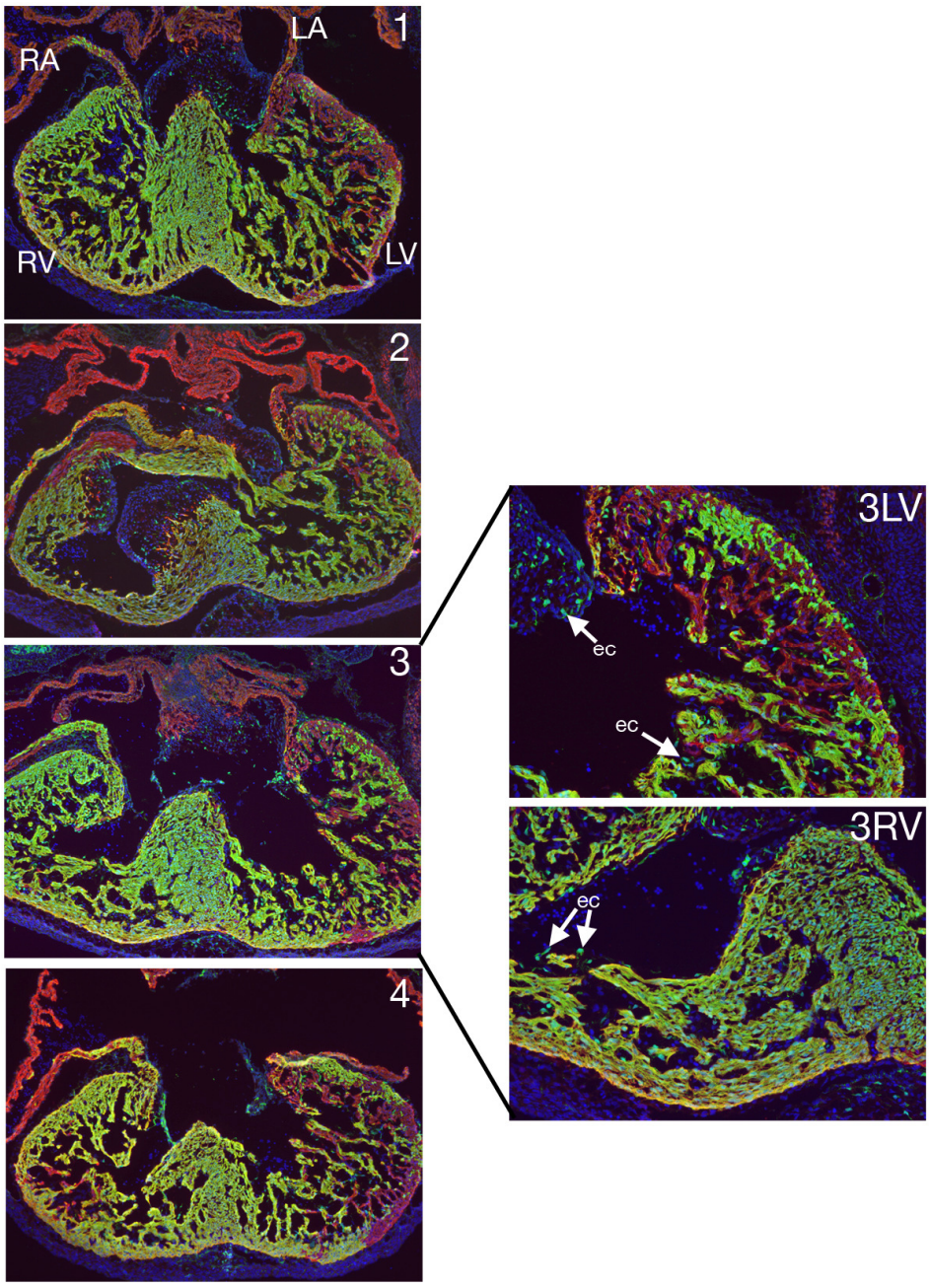

Supplementary Figure S1. Variability of Nkx2.5::Cre activity, using the RYR reporter. Sections from Nkx2.5::Cre;RYR hearts at E12.5 were immunostained for EYFP (green), alpha-tropomyosin (red), and counterstained for DAPI (blue). Four separate hearts are shown, to illustrate common and variable pattern of recombination. Note the variability of alpha-trompomyosin-positive and EYFP-negative areas, especially in the left ventricles. Scarce EYFP+ endothelial cells (ec) are shown in high magnification views of heart #3 in the left ventricle (3LV) and right ventricle (3RV). Original magnification: 50X; higher magnification is 100X.

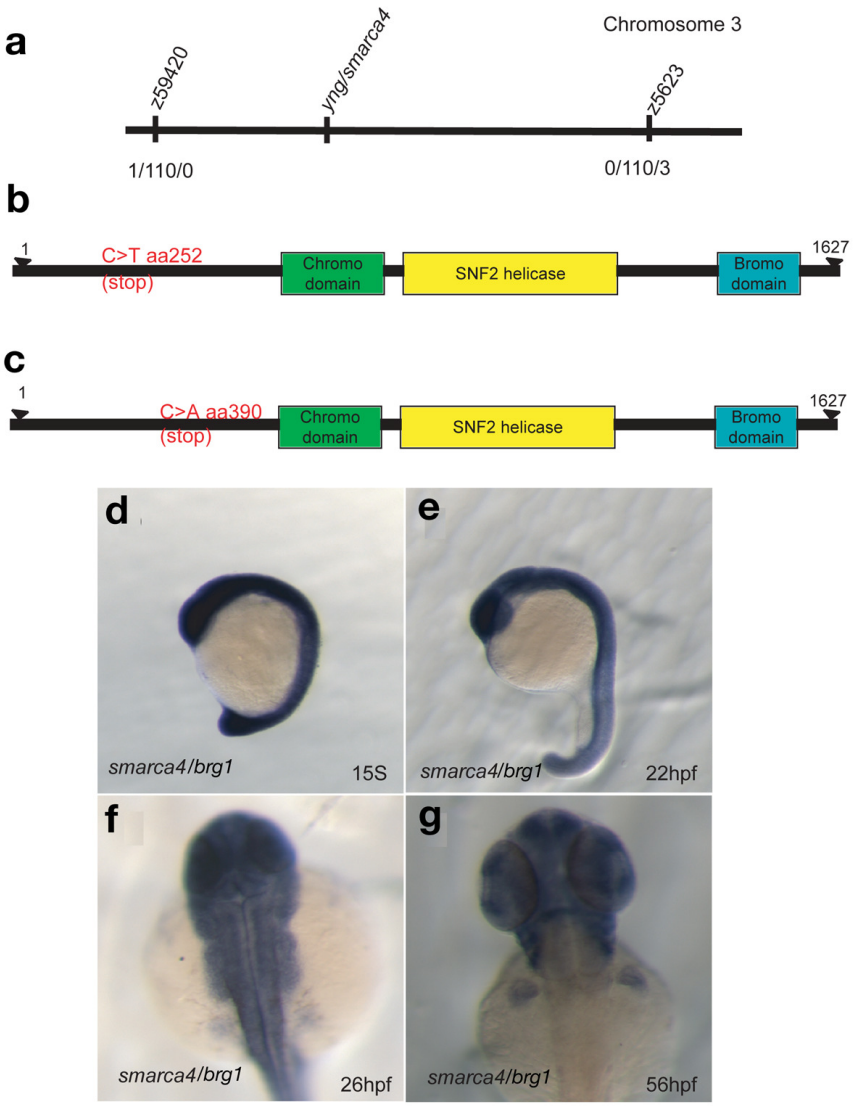

Supplementary Figure S2. Positional cloning of the *brg1*^{s481} mutation and expression of *brg1* in zebrafish embryos. **a**. The s481 lesion was mapped Chromosome 3 between markers z59420 and z5623. This region includes *smarca4/brgb*. **b**. *brg1*^{s481} mutants showed a C to T change at a position 754bp following the start of transcription, which would cause a premature stop codon following amino acid 251. **c**. The lesion observed in the original *yng*^{a8} allele. **d-g** in situ hybridization analysis of *smarca4/brg1* from 15somites to 72hpf. *smarca4/brg1* is expressed ubiquitously throughout early stages of development (**d,e**). Later expression analysis showed that *smarca4/brg1* becomes restricted to regions of the head and fin although these structures may only have increased levels (**f,g**). For **d,e,** original magnification: 100X. For **f,g,** original magnification: 200X.

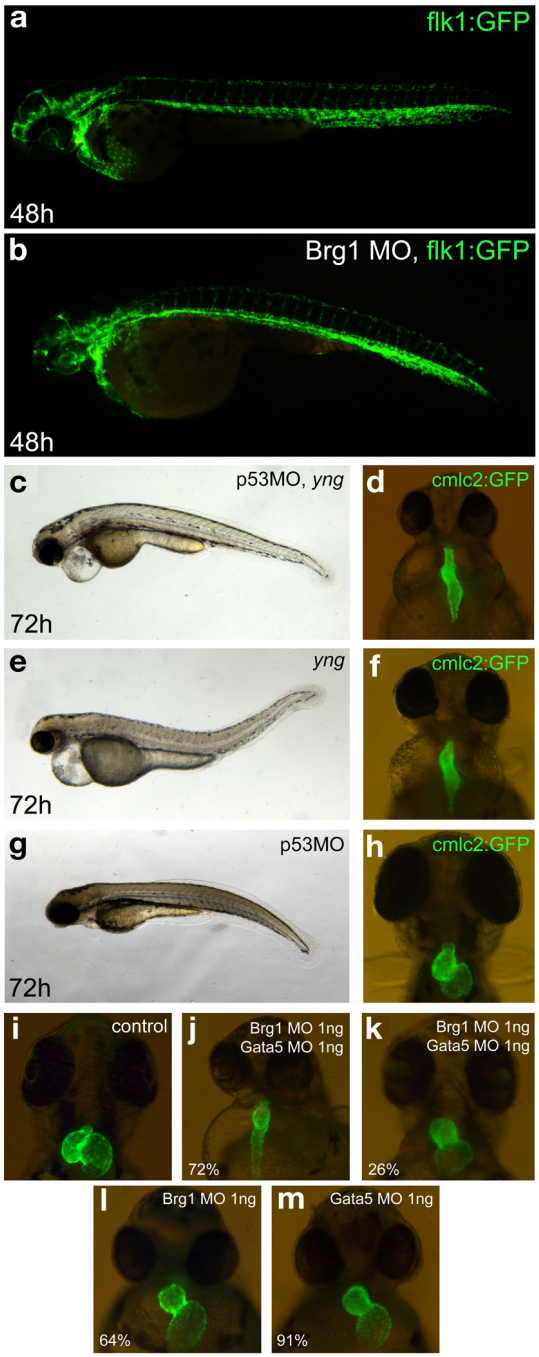

Supplementary Figure S3. **a,b,** Vascular system development in *brg1* morphant embryos. Shown are lateral view of Tg(flk1: eGFPs843) and *brg1* morphant embryo at 48hpf, anterior to left. **c-h,** Role of p53-dependent apoptosis in the brg1 phenotype. Injection of p53 morpholino in *brg1* mutant embryos (**c,d**) did not alter the brg1 mutant phenotype (**e,f**). Injection of p53 morpholino in wild type or heterozygous siblings leads no phenotype (**g,h**). **c,e,g,** lateral views; **d,f,h,** ventral views of cmlc2:eGFP transgenic embryos. **i-m,** Co-injection of *brg1* MOs and *gata5* MOs led more severe heart defects compare to single MO injection. Shown are ventral views of cmlc2:eGFP transgenic embryos. For **a-g,** Original magnification: 100X. For **h-m,** original magnification: 400X.

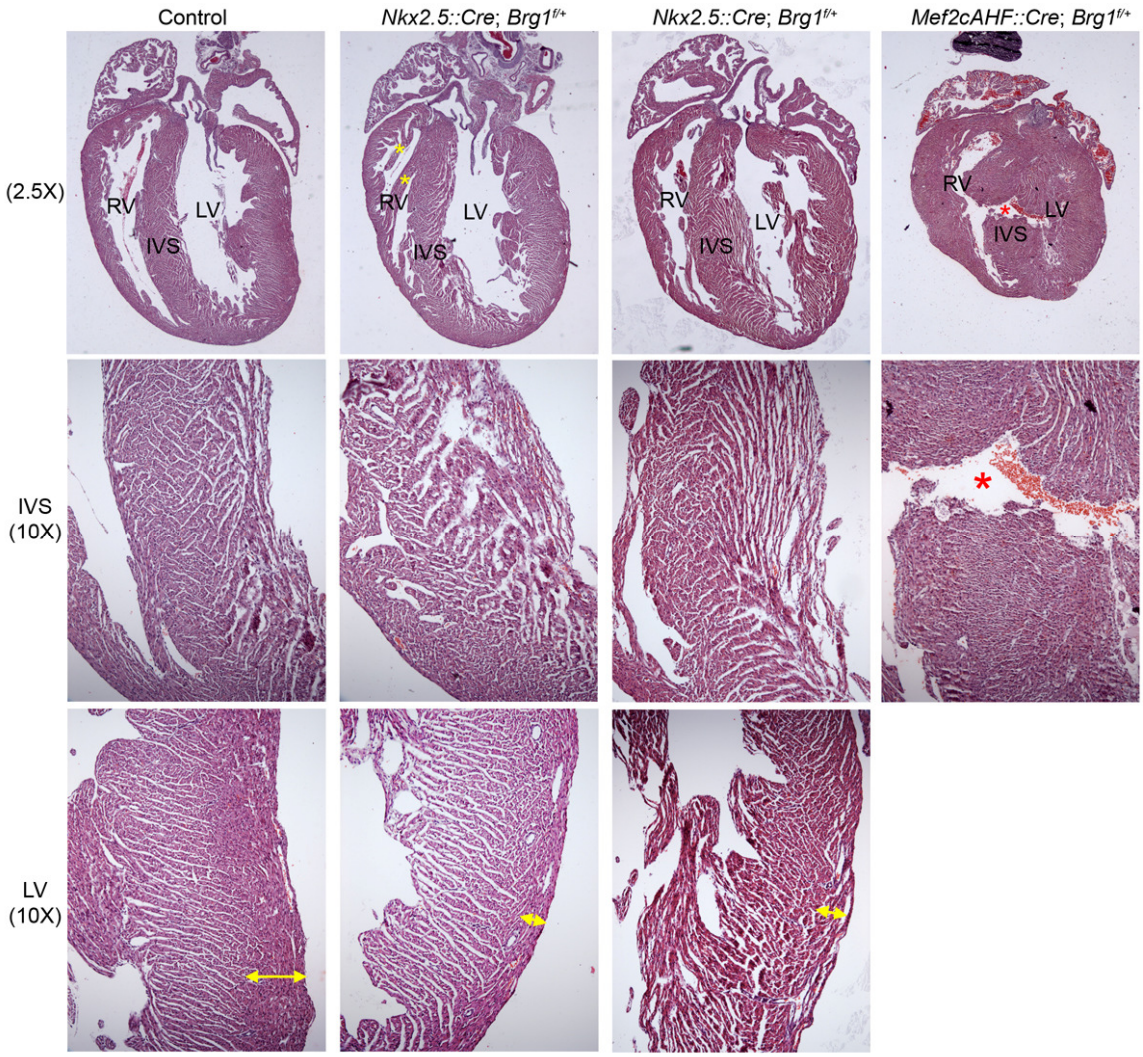

Supplementary Figure S4. Heterozygous deletion of *Brg1* using specific Cre-expressing mouse lines. Shown are hematoxylin and eosin-stained histological sections of neonatal (P2) heart from control, *Nkx2.5::Cre;Brg1*$^{fl+}$, and *Mef2cAHF::Cre;Brg1*$^{fl+}$ mice. *Nkx2.5::Cre;Brg1*$^{fl+}$hearts have overall normal morphology, but have disorganized myocardium of the interventricular septum (IVS), reduced left ventricular (LV) compact zone width (yellow arrows), and additional tissue in the right ventricle (RV; yellow asterisks). *Mef2cAHF::Cre;Brg1*$^{fl+}$ hearts had thickened and malformed RV with a large ventricular septal defect (red asterisk). Original magnification: 25X (top row), 100X (bottom rows).

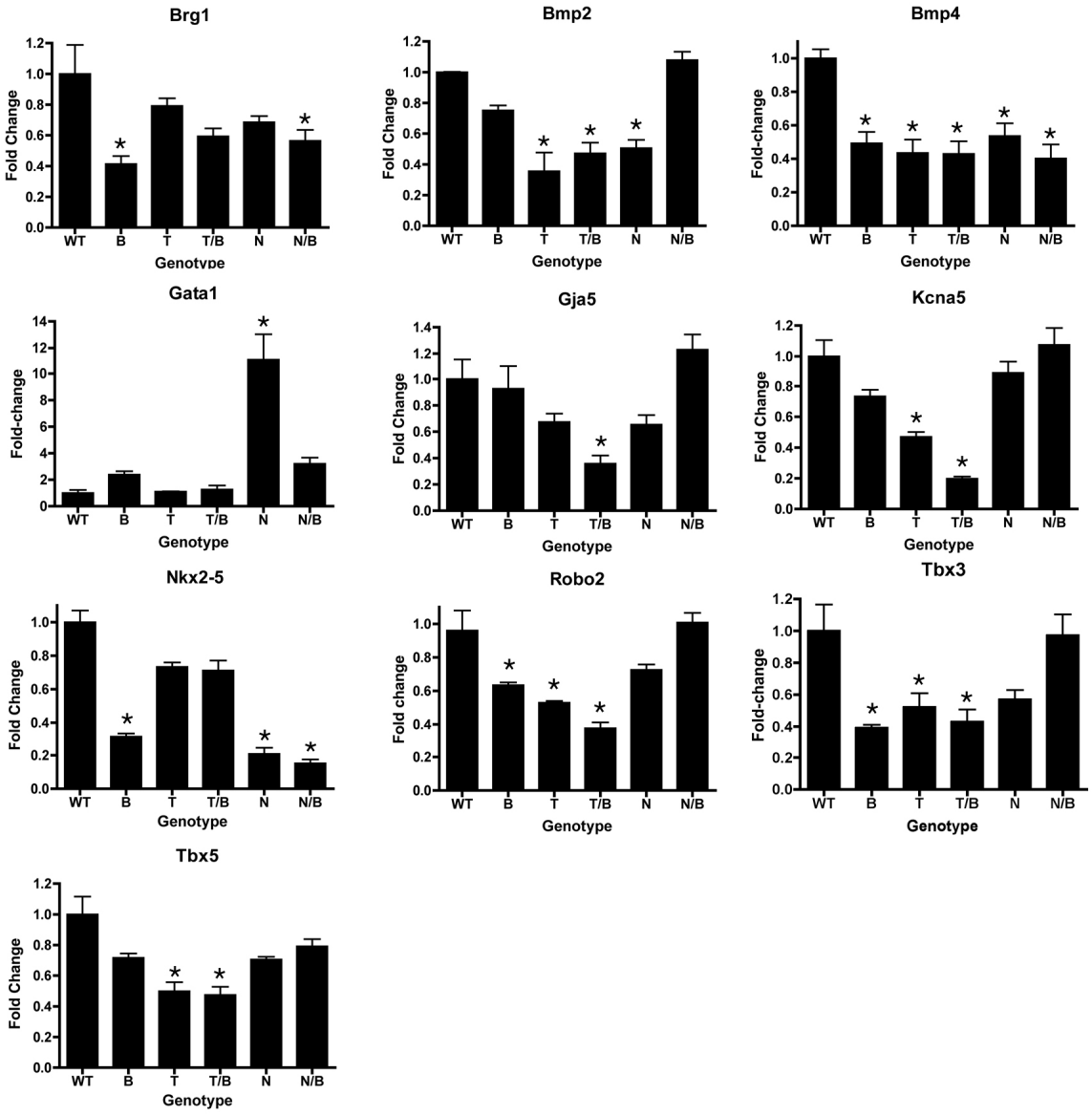

Supplementary Figure S5. Q-RT-PCR for select transcripts, as indicated above each graph. RNA was obtained from E11.5 hearts of the following genotypes: WT, *Brg1*$^{+/-}$ (B), *Tbx5*$^{del/+}$ (T), *Nkx2-5*$^{lacZ/+}$ (N), *Tbx5*$^{del/+}$;*Brg1*$^{+/-}$ (T/B), and *Nkx2-5*$^{lacZ/+}$;*Brg1*$^{+/-}$ (N/B). n=3-4. Data are mean +/- standard error. *P<0.05 vs. WT.

Supplementary Table S1: Q-PCR probesets

Gene name	Taqman probeset
Actb	Mm00607939_s1
Bmp2	Mm01340178_m1
Bmp4	Mm00432087_m1
Brg1	Mm01151944_m1
Gapdh	Mm99999915_g1
Gata1	Mm01352636_m1
Gja5	Mm00433619_s1
Kcna5	Mm00524346_s1
Nppa	Mm01151944_m1
Nkx2-5	Mm00657783_m1
Robo2	Mm00620713_m1
Tbx3	Mm00809779_s1
Tbx5	Mm00803521_m1
Wnt2	Mm00470018_m1